Vladimir Jazarević

PhD student
Universidad de Polytecnica de Catalunya
Faculty of Civil Engineering
Spain

Boško Rašuo

Full Professor
University of Belgrade
Faculty of Mechanical Engineering
Aeronautical department

Computation of Acoustic Sources for the Landing Gear During the Take-Off and Landing

The sound which is generated from the aircraft during the take-off and landing is one of the main problems for the people who live in the areas near the airport. It is very important to allocate and accurately calculate acoustic sources generated from turbulent flow produced by the aerodynamics components of the aircraft. This is done in order to calculate inhomogeneous term of Helmholtz equation which serves as a prediction tool of sound propagation in the domain. It is used subgrid-scale stabilized (SGS) finite element method for solving incompressible Navier-Stokes equation which simulate turbulent flow. Afterwards is done double divergence of Litghill's tensor in order to calculate acoustics sources. Further, the transformation from time domain to frequency domain is used with Direct Fourier Transform which leads to smaller memory usage and computational cost. The aim of the article is to show that previously mention method lead to better and richer representation of the spectrum of frequencies obtained from turbulent flow. Good representation of spectrum will give better inhomogeneous term of Helmholtz equation. Better prediction and calculation of acoustics sources will lead to reduction of sound generation through design of aerodynamics components on the aircraft.

Keywords: Aeroacoustics, turbulent flow, subgrid-scale stabilized finite element method, Litghill's analogy, Direct Fourier transform, LES method

1. INTRODUCTION

With the constant need to travel faster, better and safer through the air, the industry of aeronautics has become one of industries with the highest progression in the last century. As always progression lead to some problems that has to be overcome. One of the biggest problem for civil aviation and for people who live near the airports is sound generated from aircrafts. In one period of aviation history scientists and engineers thought that sound is coming from aircraft engine, but during 1960 Lighthill noticed that flow around aircrafts (aerodynamics) produces significant part of sound. In this period emerged a new field: Aeroacoustics. This field investigates sound generated by unsteady and/or turbulent flow and also by their interaction with solid boundaries [1]. With constant growth of capabilities of personal computers also new field of computational mechanics also emerged: Computational Aeroacoustics (CAA). The aim of this field is to simulate and predict aerodynamically generated noise. Nowadays, CAA has become an active area of research field due to its applications in the aeronautics, railway, automotive and underwater industry.

The objective of this work is to present stabilized finite element method for the approximation of incompressible Navier-Stokes equation and calculation of Lighthill's tensor which arises in Aeroacoustics for calculation of low speed CAA predictions acoustics sources. These sources are the source for the inhomogeneous Helmholtz equation which calculates distribution of pressure field in order to predict sound in domain. This work will show how different methods of stabilization for the Navier-Stokes equation gives different solution of calculation of Lighthill's tensor. The natural way to predict turbulent flow is LES (Large Eddy Simulation) [2] which would be presented in brief and compared with the proposed method of Orthogonal Subgrid-scale method (Variational multiscale method) proposed by Hughes [3]. The goal is to show how the small scales eddies have to be modelled and how they affect simulation of turbulent flow and latter calculation of aeroacoustics sources.

2. PROPOSED METHODOLOGY TO CALCULATE AEROACOUSTIC SOURCES

The first step is computational fluid dynamics (CFD) of the proposed problem. The aim of CFD is to obtain flow velocity vector $\boldsymbol{u}$, from the solution of the time evolving incompressible Navier-Stokes equation. The mathematical problem consists in solving down equation in a given computational domain $\Omega \subset \mathbb{R}^d$, with the boundary $\Gamma = \partial\Omega$ and prescribed initial and boundary condition.

$$\partial_t \boldsymbol{u} + \boldsymbol{u} \cdot \nabla \boldsymbol{u} - \upsilon \Delta \boldsymbol{u} + \nabla p = \boldsymbol{f} \quad in \, \Omega, \, t > 0, \tag{1}$$

$$\nabla \cdot \boldsymbol{u} = 0, \, in \, \Omega, \qquad t > 0, \qquad (2)$$

$$\boldsymbol{u}(x,0) = \boldsymbol{u}_0(x), in \, \Omega, t > 0, \qquad (3)$$

$$\boldsymbol{u}(x,t) = \boldsymbol{u}_D(x,t) \, on \, \Gamma_D, t > 0, \qquad (4)$$

$$\boldsymbol{n} \cdot \sigma(x,t) = \boldsymbol{t}_N(x,t) on \, \Gamma_N, t > 0, \qquad (5)$$

With υ representing the kinematic flow viscosity, $\boldsymbol{f}$ the external force and $\boldsymbol{t}_N$ the reaction on the boundary. In the case of high Reynolds number problems we will be faced with the difficulty to simulate turbulent flows. There exist mainly three options [4], namely the RANS (Reynolds Averaged Navier-Stokes equation) approach, the DNS (Direct Numerical solution) approach and the LES (Large Eddy Simulation) approach. In general, the RANS model turns to be unappropriate for aeroacoustics simulation because it cannot properly capture time fluctuations. On the other hand, DNS computational cost scales $R_e^{9/4}$, which makes it not feasible for typical high Reynolds number problems found in aeronautics. Hence, the right option is LES model and later it would be shown that proposed SGS method is even more appropriate. The second step of the simulation consists in obtaining the acoustic source term or Lighthill's tensor $\rho_0 (\nabla \otimes \nabla) : (\boldsymbol{u} \otimes \boldsymbol{u})$ from the flow velocity vector $\boldsymbol{u}$ which has already been computed in the solution of the Navier-Stokes equation.

$$(\nabla \otimes \nabla) : \boldsymbol{T} \approx \rho_0 (\nabla \otimes \nabla) : (\boldsymbol{u} \otimes \boldsymbol{u}) =$$
$$= \rho_0 \nabla \cdot [(\nabla \otimes u) \cdot u + u (\nabla \cdot u)]$$
$$= \rho \nabla \cdot [(\nabla \otimes u) \cdot u] =$$
$$= \rho u \cdot \nabla (\nabla \cdot u) + \varphi_0 (\nabla \otimes u) : (\nabla \otimes u)^T =$$
$$= \varphi_0 (\nabla \otimes u) : (\nabla \otimes u)^T = s(x,t) \qquad (6)$$

This approximation allows the direct visualization of the source term while keeping the advantages of using C^0–class finite elements. The second step of simulation finishes with performing the time Fourier transform using DFT (Direct Fourier Transform) which saves a lot of memory storage.

2.1 LES: Large Eddy Simulation

The key idea of standard LES is to decompose the velocity and pressure fields at the continuum level, so that $[\boldsymbol{u}, p] = [\overline{\boldsymbol{u}}, \overline{p}] + [\boldsymbol{u}', p']$ and the $[\overline{\boldsymbol{u}}, \overline{p}]$ representing the large scales of the flow that can be computed, whereas $[\boldsymbol{u}', p']$ counts for the non-resolvable small scales. The key point in LES [5] consist in properly modelling the effects of the non-computable small scale into the large ones. The scale decomposition between large and small scales has been done traditionally by means of a filtering process [4]. Without detailing the possible low-pass filter operations and assuming that the filter commutes with the differential operators, we can filter the Navier-Stokes equation (1)-(5) to obtain the system

$$\partial_t \overline{\boldsymbol{u}} + \overline{\boldsymbol{u}} \cdot \nabla \overline{\boldsymbol{u}} - \upsilon \Delta \overline{\boldsymbol{u}} + \nabla \overline{p} = \boldsymbol{f} - \nabla \cdot \mathcal{R} \quad in \, \Omega x(0,T) \quad (7)$$

$$\nabla \cdot \overline{\boldsymbol{u}} = 0, \, in \, \Omega x(0,T), \qquad (8)$$

$$\overline{\boldsymbol{u}}(x,0) = \overline{\boldsymbol{u}}_0(x), \, in \, \Omega \qquad (9)$$

In (7) the tensor $\mathcal{R} = \overline{\boldsymbol{u} \otimes \boldsymbol{u}} - \overline{\boldsymbol{u}} \otimes \overline{\boldsymbol{u}}$ is known as residual stress tensor, subscale tensor or subgrid scale tensor. In order for (7)-(9) to be a closed system of equations for $[\overline{\boldsymbol{u}}, \overline{p}]$. is need to express $\mathcal{R}$ in terms of $\overline{\boldsymbol{u}}$ The various choices for $\mathcal{R}$ give place to different LES models. Here is chosen Helmhotz filter that obtain $\overline{\boldsymbol{u}}$ from the solution of the Helmholtz equation $\overline{\boldsymbol{u}} - \epsilon^2 \Delta \overline{\boldsymbol{u}} = \boldsymbol{u}$. It follows that $\overline{\boldsymbol{u}} = (I - \epsilon^2 \Delta)^{-1} \boldsymbol{u}$ with $\epsilon > 0$ standing for the cut-off scale [6]. Inserting these relations into the subgrid scale tensor we obtain

$$\mathcal{R}_{ij} = \overline{(\overline{\boldsymbol{u}}_i - \epsilon^2 \Delta \overline{\boldsymbol{u}}_i)(\overline{\boldsymbol{u}}_j - \epsilon^2 \Delta \overline{\boldsymbol{u}}_j)} - \overline{\boldsymbol{u}}_i \overline{\boldsymbol{u}}_j$$
$$= 2\epsilon^2 \overline{\nabla \overline{\boldsymbol{u}}_i \cdot \nabla \overline{\boldsymbol{u}}_j} + \epsilon^4 \overline{\Delta \overline{\boldsymbol{u}}_i \Delta \overline{\boldsymbol{u}}_j} \qquad (10)$$

The expression effectively allows to write $\mathcal{R}$ in terms of $\overline{\boldsymbol{u}}$ without making any approximation or adding some hypothesis. As we will see later LES model has some drawbacks. It is not fully clear what should be characteristic of a good LES model [7] (apart from the obvious fact that it should properly reproduce experimental data). Another important question concerns the relation/interaction between arising from the physical LES model [8] and from numerical methods used to solve the discretized problem. It is also not clear what should be the relation between the filter support ϵ and the characteristic mesh element size h [9].

2.2 Subgrid scale stabilised finite element method with quasi static and dynamical subscales

To apply the SGS stabilised finite element method we will decompose the velocity and velocity test function $\boldsymbol{u} = \boldsymbol{u}_h + \tilde{u}$, $\boldsymbol{v} = \boldsymbol{v}_h + \tilde{v}$ which correspond to the space splitting $V_0^d = V_{h,0}^d \oplus V_0^d$. The velocity time derivative can be split as $\partial_t \boldsymbol{u} = \partial_t \boldsymbol{u}_h + \partial_t \tilde{u}$. The first term in previous equation would be the only one kept if the time derivative of the subscales is neglected. In this situation the subscales are termed as quasi-static [10]. If the second term is kept, the subgrid scales are termed as dynamical subsales. We will decompose the pressure and the pressure test function as $p = p_h + \tilde{p}$, $q = q_h + \tilde{q}$ corresponding to the space splitting $Q_0 = Q_{h,0} \oplus Q_0$. where $\boldsymbol{u}_h$, p_h belong to the finite element space and $\tilde{u}$ and $\tilde{p}$ are what we will call the subgrid scale. For simplicity, we will not consider pressure subscales, thus we consider $\boldsymbol{u}_* = \boldsymbol{u}_h + \tilde{u}$, $p \approx p_h$. Inserting this splitting in Galerkin formulation (multiplying with test function and integrating over hole domain) yields to:

$$(\partial_t \boldsymbol{u}_h, \boldsymbol{v}_h) + (\boldsymbol{u}_* \cdot \nabla \boldsymbol{u}_h, \boldsymbol{v}_h) + \upsilon(\nabla \boldsymbol{u}_h, \nabla \boldsymbol{v}_h) - (p_h, \nabla \cdot v_h) + (q_h, \nabla u_h)$$

$$+ (\partial_t \tilde{u}, \boldsymbol{v}_h) - \sum_K \langle \tilde{u}, \boldsymbol{u}_* \cdot \nabla \boldsymbol{v}_h + \upsilon \Delta \boldsymbol{v}_h + \nabla q_h \rangle_K$$

$$+ \sum_K \langle \tilde{u}, \upsilon \boldsymbol{n} \cdot \nabla \boldsymbol{v}_h + q_h \, n \rangle_{\partial k} = (\boldsymbol{f}, \boldsymbol{v}_h) \qquad (11)$$

$$\left(\partial_t\tilde{u},\tilde{v}\right)+\sum_K\left\langle u_*\cdot\nabla\tilde{u}-\upsilon\Delta\tilde{u},\tilde{v}\right\rangle_K+\sum_K\left\langle\upsilon\,\boldsymbol{n}\cdot\nabla\tilde{u},\tilde{v}\right\rangle$$

$$+\sum_K\left\langle\partial_t\boldsymbol{u}_h+\boldsymbol{u}_*\nabla\boldsymbol{u}_h-\upsilon\Delta\boldsymbol{u}_h+\nabla p_h,\tilde{v}\right\rangle$$

$$\sum_K\left\langle\upsilon\,\boldsymbol{n}\cdot\nabla\boldsymbol{u}_h-p_h\boldsymbol{n},\tilde{v}\right\rangle \quad (12)$$

Where equation (11) corresponds to the large scales and equation (12) corresponds to the small scales. Assuming that the velocity subscales will be zero at the element boundaries as well as on $\partial\Omega$, this allows to understand the velocity subscales as bubble function vanishing on inter element boundaries. Applying these assumptions in equation (11) leads to equation for large scales

$$(\partial_t u_h,v_h)+\left\langle u_h\cdot\nabla u_h,v_h\right\rangle+\upsilon(\nabla u_h,\nabla v_h)-$$
$$-(p_h,\nabla\cdot v_h)+(q_h,\nabla\cdot u_h)$$
$$-\sum_{\Omega_e}\left\langle\tilde{u},\upsilon\Delta v_h+u_h\cdot\nabla v_h+\nabla q_h\right\rangle_{\Omega_e}$$
$$+(\delta_t\tilde{u},v_h)+\left\langle\tilde{u}\cdot\nabla u_h,v_h\right\rangle-\left\langle\tilde{u}\cdot\nabla v_h\right\rangle=l(v) \quad (13)$$

The first line contains the Galerkin terms. The second line corresponds to terms that are already obtained in stabilization of the linearized and stationary version of the Navier-Stokes equation. It is well known that the inclusion of these terms in the formulation allow to circumvent the convection instabilities and to use equal interpolation for the velocity and the pressure fields. The third and fourth lines contain terms arising from the effects of the velocity subscales $\tilde{u}$ n the material derivative of the equation. The first term in the third accounts for the time derivatives of the subscales and the appearance of this term will distinguish method with dynamical subscales from method with quasi-static subscales, while we will justify that the second term provides global momentum conservation which is not satisfied in Galerkin finite element approach. The fourth line corresponds to a Reynolds stress for subscales. It would be explained that this term may be identified with the direct effects of the subscale turbulence onto the large scales. The key point of formulation in (13) that distinguish it from the standard SGS approach that resulted in the appearance of the additional third and fourth lines in (13) has been to keep all terms associated to the effects of the velocity subscales u in the material derivative of the exact velocity field.

$$\frac{D}{Dt}u=\frac{D}{Dt}\left(u_h+\tilde{u}\right)=$$
$$=\partial_t u_h+\partial_t\tilde{u}+\tilde{u}\cdot\nabla u_h+u_h\cdot\nabla u_h+\tilde{u}\cdot\nabla\tilde{u}+u_h\cdot\nabla\tilde{u} \quad (14)$$

Note that $\partial_t\boldsymbol{u}_h$ and $u_h\cdot\nabla u_h$ once discretized in time appear in the Galerkin formulation and the last term in (14), contributes to the standard SGS stabilisation in (13). The remaining terms $\partial_t\tilde{u}$ $\tilde{u}\cdot\nabla u_h$ and $\tilde{u}\cdot\nabla\tilde{u}$ are the new terms respectively accounting for the time dependence of the velocity subscales, momentum conservation and the subscale Reynolds stresses. Our

aim is to find now the solution in (13). Obviously to do so we first need a value for the subscales $\tilde{u}$ hat has to be obtained from the solution of the small subgrid scales equation of the problem. This equation can be written in differential form as

$$\delta_t\tilde{u}+\left(u_h+\tilde{u}\right)\cdot\nabla\tilde{u}-\upsilon\Delta\tilde{u}+\nabla\tilde{p}=r_{u,h} \quad (15)$$

with $r_{u,h}$ representing residual of the finite element components u_h given by

$$r_{u,h}=\mathcal{P}[\delta_t\tilde{u}+\left(u_h+\tilde{u}\right)\cdot\nabla\tilde{u}-\upsilon\Delta\tilde{u}+\nabla\tilde{p}-f] \quad (16)$$

It would refer to the case $\mathcal{P}=\mathcal{I}$ (entity) [4] as the Algebraic Subgrid Scale (ASGS) method, whereas $\mathcal{P}=\mathbb{P}_h=\mathcal{I}-\mathbb{P}_*$, standing for the L2 projection onto the appropriate velocity or pressure finite element space leads to the Orthogonal Subscale Stabilisation (OSS) approach. Using arguments based on a Fourier analysis for the subscale [11], the system of equation (15)-(16) can be approximated as

$$\partial_t\tilde{u}+\frac{1}{\tau_1}\tilde{u}=r_{u,h} \quad (17)$$

where the stabilisation parameter τ_1 have the expression

$$\tau_1=(c_1\frac{\upsilon}{h^2}+c_2\frac{|u_h+\tilde{u}|}{h})^{-1} \quad (18)$$

c1 and c2 in (18) are algorithmic parameters with recommended values of c1=4 and c2=2 for linear elements, while h stands for a characteristic mesh element size. From a physical point of view, the approximation (17) to problem (15) ensures that the kinetic energy of the modelled subscales resembles the kinetic energy of the exact subscales. Before we write the final equation, we will obtain essential approximation which states:

$$\sum_K\left\langle u_*\cdot\nabla\tilde{u}-\upsilon\Delta\tilde{u},\tilde{v}\right\rangle_K\approx\sum_K\tau_1^{-1}\left\langle\tilde{u},\tilde{v}\right\rangle_K \quad (19)$$

The approximations described allow us to formulate a method that can be effectively implemented and that is the formulation we propose. It consists in finding $u_h\in L^2(0,T;V_h)$ and $p_h\in D(0,T;Q_h)$ such that

$$\left(\partial_t\boldsymbol{u}_h,v_h\right)+\left(\boldsymbol{u}_*\cdot\nabla\boldsymbol{u}_h,v_h\right)+\upsilon\left(\nabla\boldsymbol{u}_h,\nabla\mathbf{v}_h\right)-$$
$$-(p_h,\nabla\cdot v_h)+(q_h,\nabla u_h)+$$
$$\sum\left\langle\tilde{u},u_*\cdot\nabla v_h+\upsilon\Delta v_h+\nabla p_h\right\rangle_{\Omega_e}=(f,v_h) \quad (21)$$
$$\left(\partial_t\tilde{u},\tilde{v}\right)+\sum\tau_K^{-1}\left\langle\tilde{u},\tilde{v}\right\rangle_{\Omega_e}$$
$$\sum\left\langle u_*\cdot\nabla u_h-\upsilon\Delta u_h+\nabla p_h,\tilde{v}\right\rangle=(f,\tilde{v}) \quad (22)$$

2.3 Conservation of momentum

Let's start analysing the effect of $\left\langle\tilde{u}\cdot\nabla u_h,v_h\right\rangle$, let V_h^d be the velocity finite element space without imposing

Dirichlet boundary conditions, that is with degrees of freedom also associated to the boundary nodes. Let t be the stress vector (traction) on the boundary Γ and consider the following augmented problem instead of (13)

$$\left(\partial_t u_h, v_h\right) + \upsilon\left(\nabla u_h, \nabla v_h\right) + \left\langle u_h \cdot \nabla u_h, v_h\right\rangle$$
$$\left(p_h, \nabla \cdot v_h\right) + \left(q_h, \nabla \cdot u_h\right) - \left(u_h, f\right) - \left\langle v_h, t\right\rangle_\Gamma$$
$$+ \left(\partial_t \tilde{u}, v_h\right) + \left\langle \tilde{u} \cdot \nabla, v_h\right\rangle - \left\langle \tilde{u}, \tilde{u} \cdot \nabla v_h\right\rangle$$
$$- \sum_K \left\langle \tilde{u}, \upsilon \Delta v_h + u_h \cdot \nabla v_h + \nabla q_h\right\rangle_K = 0 \qquad (23)$$

where now $v_h \in V_h^d$ not just $V_{h,0}^d$. Considering d=3 and taking for example v_h 1,0,0) and q_h, this equation yields

$$\int_\Omega \left[\partial_t\left(u_{h,1} + \tilde{u}_1\right) - u_{h,1} \nabla \cdot u_h\right] d\Omega + \int_\Omega \tilde{u} \cdot \nabla u_{h,1} d\Omega +$$
$$+ \int_\Gamma u_{h,1} u_n \cdot n d\Gamma = \int_\Gamma f_1 d\Gamma + \int_\Gamma t_1 d\Gamma \qquad (24)$$

where now the zero Dirichlet conditions for the velocity is not explicitly required. This statement provides global momentum conservation if

$$-\int_\Omega u_{h,1} \nabla \cdot u_h d\Omega + \int_\Omega \tilde{u} \cdot \nabla u_{h,1} d\Omega = 0 . \qquad (25)$$

This is implied by the continuity equation obtained by taking

$$\left(q_h, \nabla \cdot u_h\right) - \sum_K \left\langle \tilde{u}, \nabla q_h\right\rangle_K = 0 . \qquad (26)$$

provided $V_h / R \subseteq Q_{h,0}$ that is to say, the velocity component $u_{h,1}$ belongs to the pressure space ($u_{h,1}$ can be considered modulo constants) This holds for natural choice $V_h / R = Q_{h,0}$, that is to say, equal velocity-pressure interpolations. For the standard Galerkin method, this condition is impossible to be satisfied, since equal interpolation does not satisfy the inf-sup condition. As a conclusion the term $\tilde{u} \cdot \nabla, v_h$ provides global momentum conservation, since without it in discrete momentum equation, we would have obtained

$$-\int_\Omega u_{h,1} \nabla \cdot u_h d\Omega = 0 .$$

instead of (25), which is not implied by (26).

2.4 Door to turbulece

Let us make some speculative comments on the possibility to simulate turbulent flows using the formulation in (44) and on the role of the remaining term $-\left\langle \tilde{u}, \tilde{u} \cdot \nabla v_h\right\rangle$. In standard LES approach the tensor $\mathcal{R}$ s often decomposed into the so-called Reynolds, Cross and Leonard stresses to keep the

Galiean invariance of the original Navier-Stokes equation. This invariance is automatically inherited by the formulation presented above and we observe that analogous term so the various stress types are recovered in a natural way from our pure numerical approach

$$-\left\langle \tilde{u}, \tilde{u} \cdot \nabla v_h\right\rangle = -\left\langle \tilde{u} \otimes \tilde{u}, \nabla v_h\right\rangle \text{ (Reynolds stress)} (27)$$

while the addition of the other three terms becomes, after integration by parts.

$$\left\langle u_h \cdot \nabla u_h, v_h\right\rangle - \left\langle \tilde{u}, u_h \cdot \nabla v_h\right\rangle + \left\langle \tilde{u} \cdot \nabla u_h, v_h\right\rangle =$$
$$-\left\langle u_h \otimes u_h, \nabla v_h\right\rangle \text{ (Convection of large scales)}$$
$$-\left\langle u_h \otimes \tilde{u} + \tilde{u} \otimes u_h, \nabla v_h\right\rangle \text{ (Cross stress)} \qquad (28)$$

If we now pay attention to the convective term of the residual in the subscale equation (17) and take for simplicity the Algebraic subscale projection, we observe that

$$\left\langle (u_h + \tilde{u}) \cdot \nabla u_h, \tilde{v}\right\rangle =$$
$$-\left\langle u_h \otimes u_h, \nabla \tilde{v}\right\rangle - \left\langle u_h \otimes \tilde{u}, \nabla \tilde{v}\right\rangle \text{ (Leonard stress)} (29)$$

Hence, we can effectively conclude that the modifications introduced by the presence of the divergence of $\mathcal{R}$. In the LES approach are somehow automatically included in our subgrid scale stabilized finite element approach. In the present formulation the remaining Reynolds stress term (27), is then considered to account for the direct subscale turbulent effects onto the large, resolvable, scales. However, all terms involving the subscales are indirectly affected by the turbulence effects because the subscales are obtained from the non-linear equation (17) that involves (29).

2.5 Energy balance equation for Navier-Stokes problem

Navier-Stokes equations have been stated in (1)-(5). It can be rewritten in conservative form using strain tensor $S(u) = \frac{1}{2}(\nabla u + \nabla u^T)$ we could formulate the weak form as: find $[u, p] \in L^2(0, T; H_0^1(\Omega)) x L^1(0, T; L^2(\Omega) / R)$ such that

$$\left(\partial_t u, v\right) + 2\upsilon\left(S(u), S(v)\right) + \nabla \cdot \left(u \otimes u\right), v - \left(p, \nabla \cdot v\right) = \left\langle f, v\right\rangle$$
$$\left(q, \nabla \cdot u\right) = 0 \qquad (30)$$

From which we obtain the energy balance equation

$$\frac{d}{dt}\left(\frac{1}{2} u^2\right) = -2\upsilon S(u)^2 + \left\langle f, u\right\rangle \qquad (31)$$

Equation (28) states that the time variation of the flow kinetic energy depends on two factors, namely, the molecular dissipation due to viscosity (clearly negative) and the power exerted by the external force that can be either positive or negative. Previous equation could be rewritten as

$$\int_{\Omega} \frac{dk}{dt} d\Omega = -\int_{\Omega} \epsilon_{mol} d\Omega + \int_{\Omega} P_f d\Omega \qquad (32)$$

According to the Kolmogorov description of the energy cascade in turbulent flows, the flow can be viewed as driven by the external forces acting at the large scales (high wave numbers) by non-linear processes. When the Kolmogorov length is reached, the viscous dissipation ϵ_{mol} in the r.h.s of (32) takes part transforming the flow kinetic energy into internal energy (heat released).

2.6 Energy balance equation for Large Eddy simulation model

Considering the same assumptions used to derive (7)-(9), we get the weak form of filtered incompressible Navier-Stokes equation in a conservative form:

$$\left(\partial_t \overline{u}, v\right) + 2\upsilon\left(S\left(\overline{u}\right), S\left(v\right)\right) + \left(\nabla \cdot \left(\overline{u} \otimes \overline{u}\right), v\right)$$
$$-\left(\overline{p}, \nabla \cdot v\right) = \left(\overline{f}, v\right) + \left(\mathcal{R}, \nabla v\right) \qquad (33)$$
$$\left(q, \nabla \cdot \overline{u}\right) = 0 \qquad (34)$$

Taking in to account that $\mathcal{R}$ is symmetric, we can rewrite the second term in the r.h.s of (33). As $\left(\mathcal{R}, \nabla v\right) = \left(\mathcal{R}, S(v)\right)$ we will consider $\mathcal{R}$ deviatoric, where its volumetric part being absorbed in the pressure term it could be written energy balance equation for filtered Navier-Stokes equation:

$$\frac{d}{dt}\left(\frac{1}{2}\overline{u}^2\right) = -2\upsilon S(\overline{u})^2 + \mathcal{R}, S(\overline{u}) + \left\langle \overline{f}, \overline{u} \right\rangle \qquad (35)$$

where we could rewrite this equation assuming that the rate of production of residual kinetic energy $\overline{P}_r = -\mathcal{R} : S(\overline{u})$.

$$\int_{\Omega} \frac{d\overline{k}}{dt} d\Omega = -\int_{\Omega} \overline{\epsilon}_{mol} d\Omega - \int_{\Omega} \overline{P}_r d\Omega + \int_{\Omega} \overline{P}_f d\Omega \qquad (36)$$

For a fully developed turbulent flow with the filter width in the inertial sub range, the filtered fields account for almost all the kinetic energy of the flow thus $\int_{\Omega} \frac{d\overline{k}}{dt} d\Omega \approx \int_{\Omega} \frac{dk}{dt} d\Omega$. If the external force acts mainly on the large scales of the flow, it would also happen that third term on r.h.s of (35) is equal to third term of r.h.s of (36). On the other hand, the energy dissipated by the filtered field $\overline{\epsilon}_{mol}$ is relatively small and can be neglected. Consequently, comparing equation (32) with (36) we observe that in order for the LES model to behave correctly it should happen that

$\int_{\Omega} \overline{P}_r d\Omega \approx \int_{\Omega} \epsilon_{mol} d\Omega$, that is, the rate of production of residual kinetic energy should be equal to (in the mean) the energy dissipated by viscous processes at the very small scales (Kolmogorov length) which is point of view expressed by Liily [8]. In the case of some celebrated LES models, such as Smagorinsky model $\overline{P}_r$, is always positive and there is no backscatter, i.e, the energy is always transferred from the filtered scales to the residual ones, but not vice versa.

2.7 Energy balance equation for SGS method with static and dynamical subscales

We will use here the orthogonal subgrid scale (OSS) approach and also quasi static subscales, because of that equation (17) and could be written as $\tilde{u} = \tau_1 r_{u,h}$, where $r_{u,h}$ represents the orthogonal projection of the residuals of the finite element component u_h and in the end equation (16) has a new form

$$r_{u,h} = -\mathbb{P}_h^{\perp}[-2\upsilon\nabla \cdot S\left(u_h\right) + \nabla \cdot \left(u_h \otimes u_h\right) + \nabla p_h] \qquad (37)$$

and stabilisation parameter τ_1 s defined as

$$\tau_1 = [\left(c_1 \frac{\upsilon}{h^2}\right)^2 + \left(c_2 \frac{|u_h|}{h}\right)^2]^{-\frac{1}{2}} \qquad (38)$$

When everything is defined we could write the energy balance equation as

$$\frac{1}{2}\frac{d}{dt}\left\|u_h\right\|^2 = -2\upsilon\left\|S\left(u_h\right)\right\|^2 -$$

$$-\sum_e \left\langle \tilde{u}, 2\upsilon\nabla \cdot S\left(u_h\right) + \nabla \cdot \left(u_h \otimes u_h\right)\right\rangle + \left\langle f, u_h \right\rangle \qquad (39)$$

The summations with index e are assumed to be extended over all elements. If we consider the subscale approximation, we obtain

$$\frac{1}{2}\frac{d}{dt}\left\|u_h\right\|^2 = -2\upsilon S(u_h)^2 + \left\langle f, u_h \right\rangle$$

$$-\sum_e \tau_1(\mathbb{P}_h^{\perp}[-2\upsilon\nabla \cdot S(u_h) + \nabla \cdot (u_h \otimes u_h)\nabla p_h]$$

$$+2\upsilon\nabla \cdot S\left(u_h\right) + \nabla \cdot (u_h \otimes u_h))_{\Omega_e} \qquad (40)$$

Since we are interested in high Reynolds numbers, all the stabilisation terms multiplied by the viscosity will be neglected, from where we obtain the following energy balance equation for the OSS stabilised finite element approach to the Navier-Stokes equations.

$$\frac{1}{2}\frac{d}{dt}\left\|u_h\right\|^2 = -2\upsilon\left\|S\left(u_h\right)\right\|^2 + \left\langle f_h, u_h \right\rangle$$

$$-\sum_e \tau_1(\mathbb{P}_h^{\perp}[\nabla \cdot (u_h \otimes u_h) + \nabla p_h], \nabla \cdot (u_h \otimes u_h))_{\Omega_e} \qquad (41)$$

We could rewrite as before in the form

$$\int_{\Omega} \frac{dk^h}{dt} d\Omega = -\int_{\Omega} \epsilon^h_{mol} d\Omega - \int_{\Omega} \mathbb{P}^{hr}_r d\Omega + \int_{\Omega} P^h_f d\Omega \qquad (42)$$

where $\mathbb{P}^{hr}_r$ is defined in second line of equation (38). It is clear that k^h will account for nearly the whole point-

wise kinetic energy of the flow so that $\int_{\Omega} \frac{dk^h}{dt} d\Omega \approx \int_{\Omega} \frac{dk}{dt} d\Omega$.

On the other hand, it will also occur that $\int_{\Omega} P_f d\Omega \approx \int_{\Omega} P_f^h d\Omega$ even that the force only acts at the large scales. In addition the numerical molecular dissipation of the large scales will be negligible, so that: $\int_{\Omega} \epsilon_h^{mol} d\Omega \approx 0$. The next, crucial question is if it should happen that $\sum_e \int_{\Omega_e} P_r^{h\tau} d\Omega \approx \int_{\Omega} \epsilon_{mol} d\Omega$ for the OSS formulation to be good numerical approach for the Navier-Stokes equations, in case of fully developed turbulence. Actually, this should not be necessarily the case for all the terms in $P_r^{h\tau}$ given that they have arisen in the equation motivated by pure numerical stabilisation necessities. However, it is clear that at least some of these terms should account for the appropriate physical behaviour and their domain integration should approximate the mean molecular dissipation in (31). It would be one of the main outcome of this article to show, by means of heuristic reasoning, that actually the whole $P_r^{h\tau}$ satisfies this assumption.

2.8 Discrete Fourier Transform

Natural choice for implementing Fourier transform on the computer is Fast Fourier transform (FFT) because of less time to compute the transformation. In our implementation we won't use FFT, Discrete Fourier Transform (DFT) would be used.

$$H\left(f_n\right) = \int_{-\infty}^{\infty} h(t)e^{-2\pi i f_n t} dt \approx \sum_{k=0}^{N-1} h_k e^{-2\pi i f_n t_k} \Delta .$$

$$= \Delta \sum_{k=0}^{N-1} h_k e^{-2\pi i k n / N} . \quad (43)$$

As it is known FFT uses some subroutines for rearranging some instance in vector numeration in order to achieve faster calculation. That means that there is need to store all velocity vectors in every time step, what is very memory space consuming in order to apply FFT. This problem will be overcome with DFT which will be implemented inside of transient loop in Navier stokes equation achieving less computational time and there is not need to store velocity vectors, they are going immediately in time numeration of DFT.

2.9 CFD simulation of generic landing gear struts with horizontal angle α=0° and rectangular cross section using LES model and SGS method with dynamical Subscales

Here, it would be presented the practical part of the article, where it would be shown CFD simulation of generic landing gear struts shown in figure 1.

For the sake of simplicity it would be simulated 2D version of simple 3D model shown in figure 2. It is assumes as two struts are of infinite third dimension and emerged in an infinite uniform flow. It is used simple

model which is used for experimental investigation as a part of the project Valiant.

Figure 1. Landing gear   **Figure 2. Simple 3D model of two struts**

We will concentrate here on the case where the flow loses its steadiness as well as its up-and-down symmetry and a wake of altering vortices are formed behind the struts. The set of these shed vortices is known as the von Karman vortex street. Vortex shedding induces lift fluctuations on the body, which leads to the radiation of sound having dipole pattern.

The configuration of struts consists of two in line square struts at the centre-to-centre distance S=0.16m. Both struts have width D=0.04m, the distributed flow speed is U0=70m/s which is imposed on the left side of the rectangle domain and the fluid is air at atmospheric pressure and ambient temperature (say 20 °C).

The mesh used to perform computation is shown in figure 3.
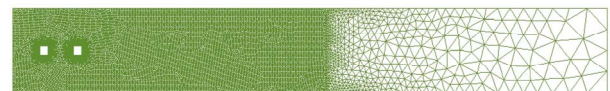
Figure 3. Mesh used for simulation
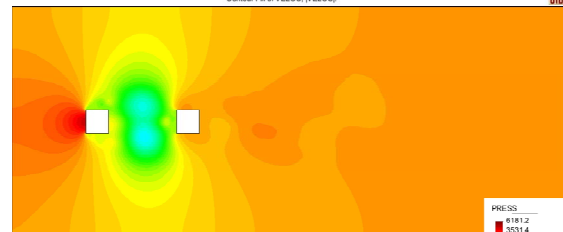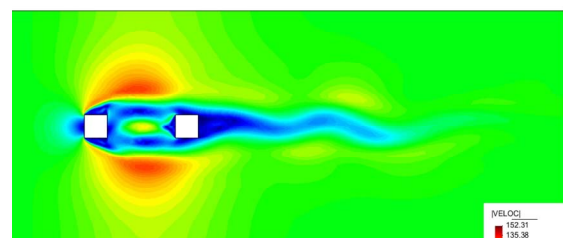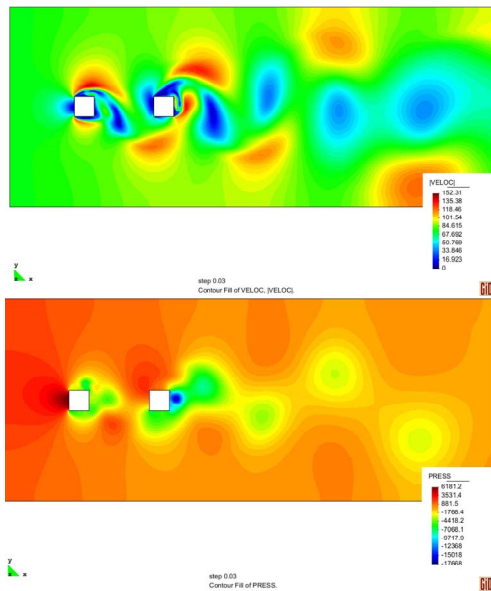
Figure 4. Velocity and pressure field using LES model
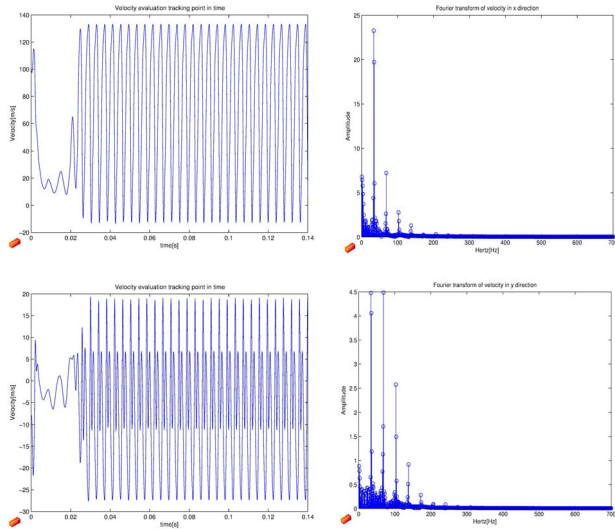
Figure 5. Velocity tracking (x and y component) in point between struts and spectral diagram of velocity obtained with LES model
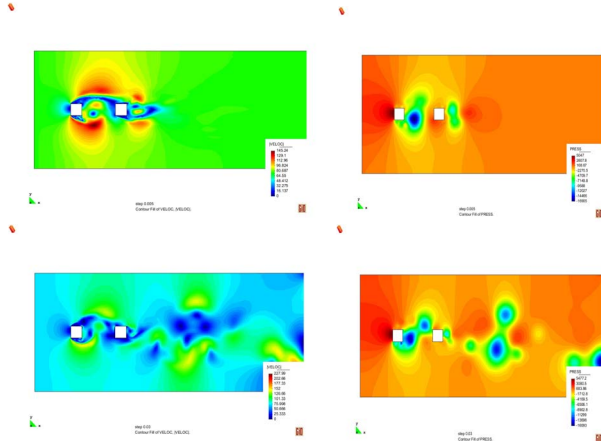
Figure 6. Velocity and pressure field using SGS with dynamical subscales

In figure 4-5 is shown velocity and pressure field using LES model. As it is clear from figure 5 that LES model has a poor spectrum diagram of frequencies which means that this model is simulating only large

scales and only small amount of small scales. Also what is obvious that this model is very dissipative because in this case the LES cannot capture real turbulent behaviour for this velocity and Reynolds number.

In figure 6-7 is shown velocity and pressure field and also velocity tracking in point between struts.

From the figure 7 Is obvious that SGS method with dynamical subscales is giving better representation of turbulent flow and also giving the richer spectral diagram recovering small fluctuations who are coming from small scales.

In the end is shown figure 8 where is shown acoustics sources for some particular frequency. Aeroacousitcs source is imaginary number and because of that is shown real and imaginary part. In the figure is recognized dipole pattern of aeroacoustics sources which is recognizable for von Karmen vortex sheding behaviour of turbulent flow.
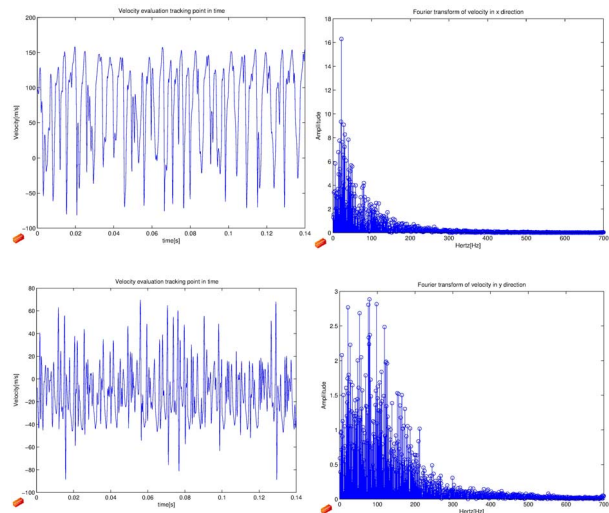
Figure 7. Velocity tracking (x and y component) in point between struts and spectral diagram of velocity obtained with SGS with dynamical subscales model
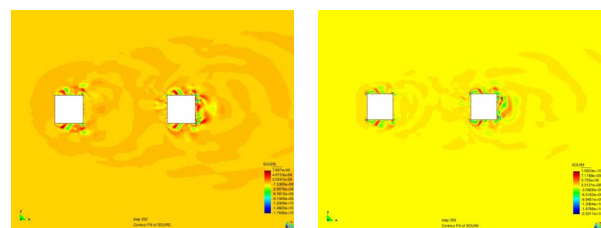
Figure 8. Dipole pattern of acoustics sources obtained from turbulent flow (real and imaginary part) using SGS with dynamical subscales

2.10 CFD simulation of generic landing gear struts with circular cross section using SGS model with dynamical subscales

In previous section are shown the struts with rectangular cross section because of easiest way to show the main thing of the new method of SGS. Also it is done because of the connection with VALIANT project where the same thing was performed aero tunnel in order to collect experimental data. Of course the rectangular cross section is not something that would be found on aircraft

landing gear and because of that here is shown the CFD simulation of two circular cross section emerged in infinite flow field where the characteristics of the flow are the same as in previous example. In figure 9. Is shown the mesh of the model.

Figure 9. Mesh used for simulation

In figure 10. is shown the velocity field of two struts of circular cross section. It could be clearly noticed the vortex shedding which is important for the generation of aeroacoustics sources.

In the end in figure 11 is shown aeroacousitcs source field on the frequency of 100Hz. The picture is zoomed for one cylinder in order to show dipole pattern which is the characteristic for vortex shedding.
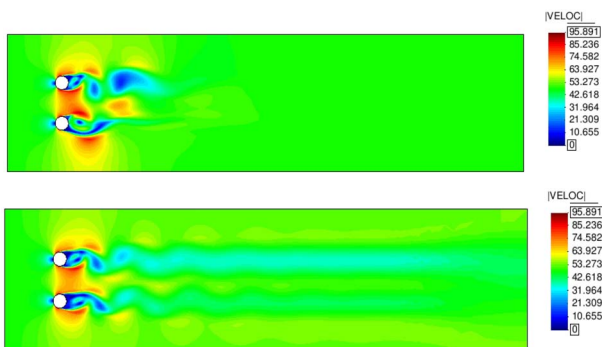
Figure 10. Velocity field for different time steps
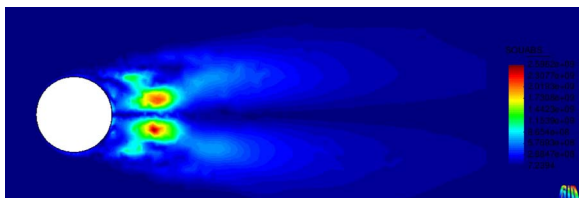
Figure 11. Aeroacoustic source on frequency f=100Hz

3. CONCLUSION

The main objective of this article was to show the advantage of using a new method of SGS with dynamical subscales. The advantage is in better representation of turbulent flow which is clearly shown in above figures. This method gives a good representation of small scales which are somehow lost in LES modelling.

Comparison is shown in previous figures what clearly shows the power of presented method.

Good approximation of small scales give richer presentation of frequencies spectrum. This frequency spectrum is a direct indicator of behaviour of turbulent flow. Better presentation of turbulent flow immediately give more accurate approximation of aeroacoustics sources. Also the improvement is madden through usage of DFT method for transition from time domain to frequency domain. DFT is implemented inside of time

loop of transient Navier-Stokes equation where this approach leads to reducing the memory usage and computational cost. The aim of future work is to show that this better approximation of aeroacoustics sources will lead to better prediction of sound propagation. This would be done through inhomogeneous Helmholtz equation. Also the idea is to use the same stabilisation method for Helmholtz equation in order to overcome the problem of pollution error for large wave numbers.

REFFERENCES

[1] Flowcs–Williams, J. and Hawkings, D.: Sound generated by turbulence and surfaces in arbitrary motion. Phil Trans Roy. Sec A, 264: 321-342, 1969.

[2] Canuto, V.: Large Eddy simulation of turbulence: a subgrid scale model including shear, vorticity, rotation and buoyancy, Astrophysical J., 428: 729-758, 1994.

[3] Hughes, T.J.R.: Multiscale phenomena: Green's function, the Dirichlet-to-Neumann formulation, subgrid scale models, bubbles and the origins of stabilized formulations, Computer Methods in Applied Mechanics and engineering, 127, pp. 387-401,1995.

[4] Pope, S.: *Turbulent flows*, Cambridge University Press, 2000.

[5] Berselli, L., Iliescu, T., and Layton, W.: *Mathematics of Large Eddy Simulation of turbulent flows*, Springer, 2006.

[6] Wagner, C., Hüttl, T. and Sagaut, P.: *Large-Eddy Simulation for Acoustics*, Cambridge Aerospace Series, Cambridge University Press, 2012.

[7] Lesieur, M., Metais, O. and Comte, P.: *Large-Eddy Simulations In Turbulence*, Cambridge University Press, 2005.

[8] Volker, J.: *Large Eddy Simulation of Turbulent Incompressible Flows: Analytical and Numerical Results for a Class of Les Models*, Springer, 2004.

[9] Germano, M.: Differential filters for the large eddy simulation of turbulent flows. Phys. Fluids, Vol. 29, No.6, pp. 1755-1757, 1986.

[10] Codina, R.: Stabilisation of incompressibility and convection through orthogonal sub-scales in finite element methods, Computer Methods in Applied Mechanics and engineering, 190, pp. 1579-1599, 1965.

[11] Lilly, D.: The representation of small-scale turbulence theory in numerical simulation experiments,Proc. IBM Scientific Computing Symp. on Environmental Science, 1967.

ПРОРАЧУН АЕРОАКУСТИЧНИХ ИЗВОРА КОЈЕ ГЕНЕРИШЕ СТАЈНИ ТРАП АВИОНА ПРИЛИКОМ СЛЕТАЊА И ПОЛЕТАЊА.

Владимир Јазаревић, Бошко Рашуо

Звук који се генерише са делова авиона приликом слетања и полетања је један од главних проблема за људе који живе у областима поред аеродрома. Веома је битно да се лоцирају и прецизно израчунају акустични извори који се генеришу из турбулентног струјања око аеродинамичких компоненти авиона. Израчунати извори су нехомогени део Хелмхолцове једначине која се користи за предвиђање пропагације звука у прорачунском домену. Коришћен је "Subgrid-scale" стабилициони метод коначних елемената за решавање некомпресибилне Навије-Стокс-ове једначине за симулацију турбулентног струјања и дупла дивергенција Litghill-овог тензора у циљу прорачуна акустичних извора. У следећем кораку прелазак из временског домена у фреквентни домен је урађен кроз директну Фуриеову трансформацију која доводи до мањег прорачунског времена и заузимања меморије. У раду је показано да споменути метод срачунава бољи и богатији спектар фреквенција које ће дати бољи и тачнији нехомогени члан Хелмхолцове једначине. Боље предвиђање и прорачун акустичних извора ће довести до редуковања генерисања звука кроз редизајн аеродинамичких компоннети на авиону.